Sex-Specific Role for SLIT1 in Regulating Stress Susceptibility

Supplement 1

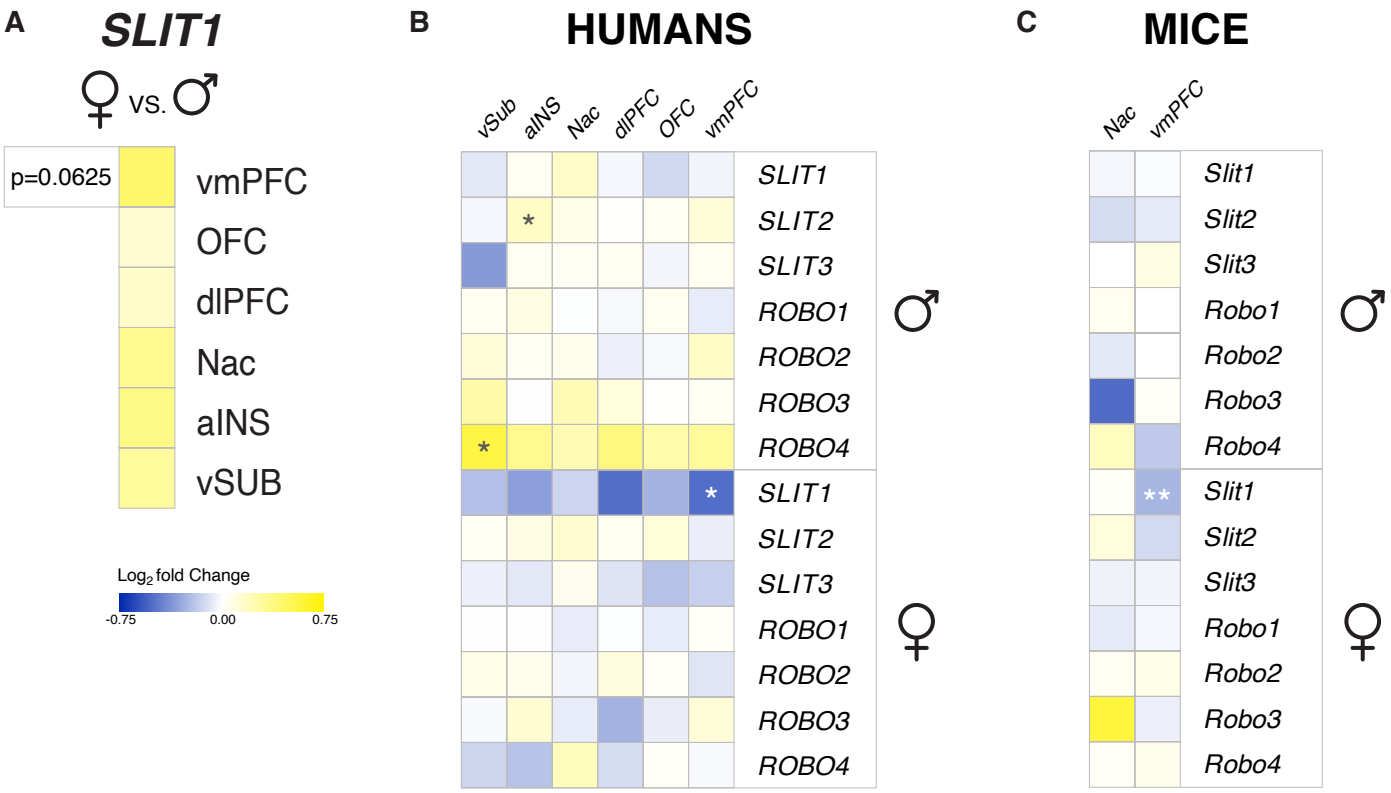

Supplemental Figure S1. Regulation of *Slit* and *Robo* family genes in depressed humans and chronically stressed mice. (A) Heatmap representing RNA-seq results showing a trend for higher levels of *Slit1* mRNA in control females compared to control males in humans. Trending effect in females vs. males vmPFC. vmPFC, ventromedial prefrontal cortex; dlPFC, dorsolateral PFC; OFC, orbitofrontal cortex; NAc, nucleus accumbens; aINS, anterior insula; and vSUB, ventral subiculum. **(B)** Heatmap of RNA-seq results showing expression levels of all *Slit* or *Robo* family members in the six brain regions of depressed males or females compared to controls in humans. **(C)** Heatmap representing RNA-seq results indicating specific downregulation of *Slit1* in the vmPFC of female mice after CVS, with no change in any other *Slit* or *Robo* family member in either the vmPFC or NAc.

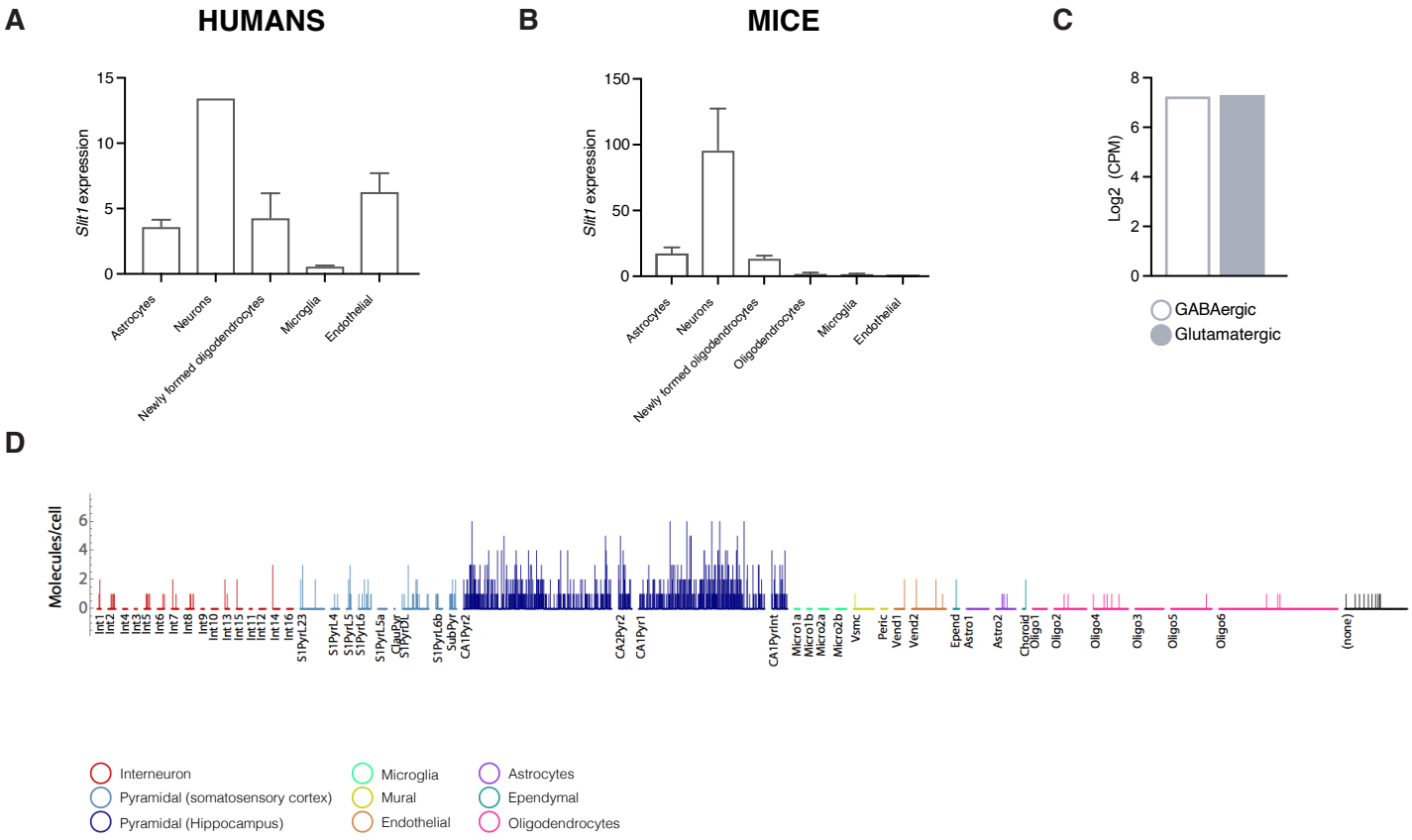

Supplemental Figure S2. *Slit1* is a neuronal gene expressed in both GABAergic and glutamatergic neurons. (A, B) Neurons show the highest expression of *Slit1* in the central nervous system in humans **(A)** and mice **(B)** compared to other cells types. (Data modified from (16, 17)). **(C)** *Slit1* is expressed in similar levels in both glutamatergic and GABAergic neurons from healthy postmortem human subjects. (Data modified from (18)). **(D)** *Slit1* shows increased intensity and expression levels in glutamatergic neurons compared to other neuron types in mouse somatosensory cortex. (Data modified from (19)). *p<0.05. Data are shown as means ± s.e.m.

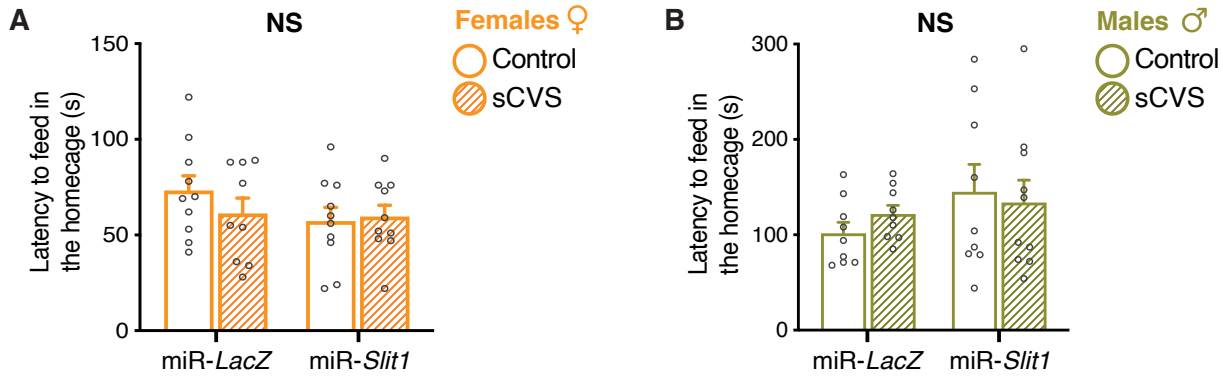

Supplemental Figure S3. *Slit1* KD had no effect on home cage latency to feed in the NSF posttest. **(A, B)** Viral manipulation had no effect on appetite in the posttest for both females **(A)** and males **(B)**.

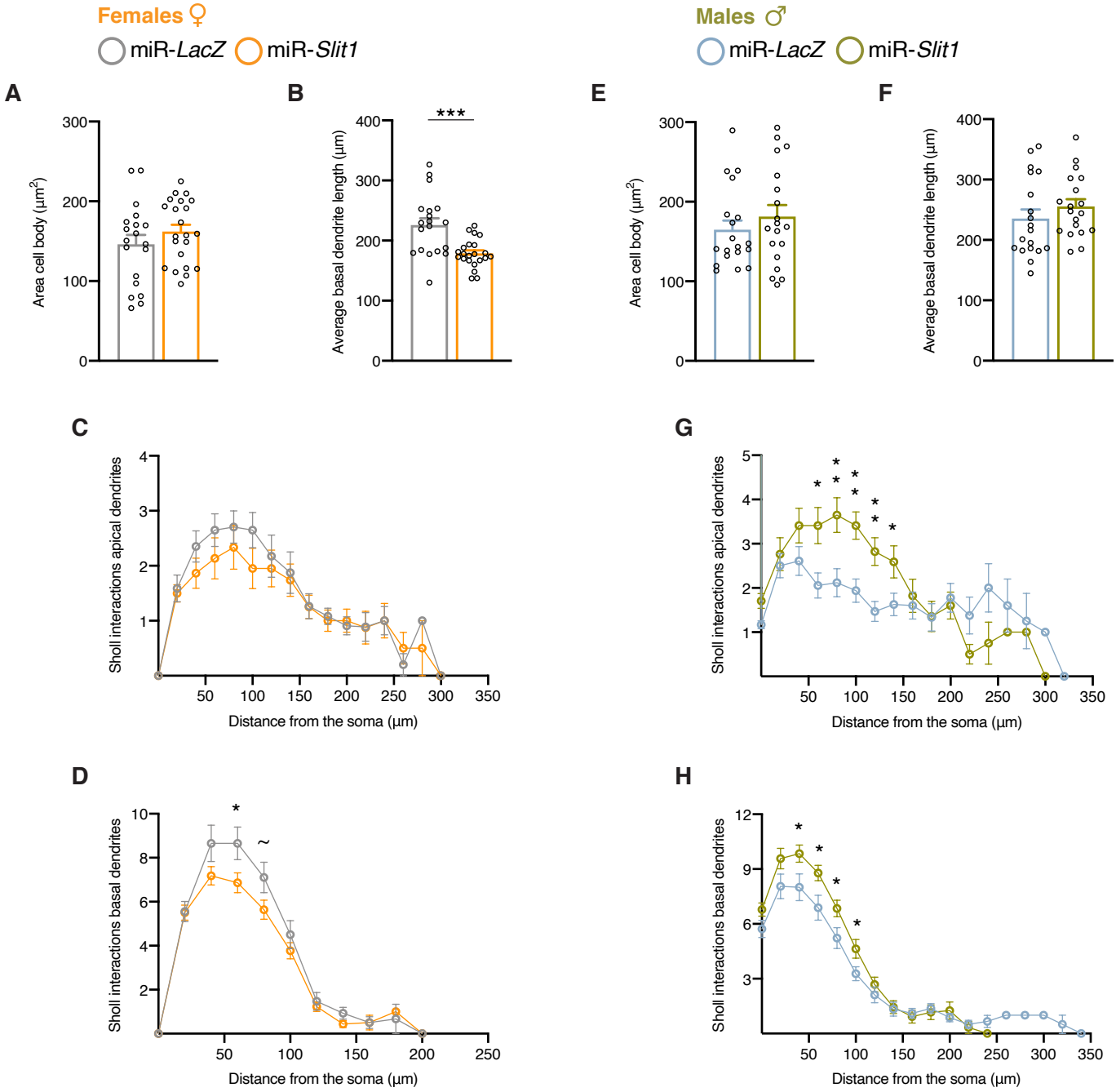
Females ♀
miR-LacZ
miR-Slit1
A
Area cell body (µm²)
B
Average basal dendrite length (µm)
***
Males ♂
miR-LacZ
miR-Slit1
E
Area cell body (µm²)
F
Average basal dendrite length (µm)
C
Sholl interactions apical dendrites
Distance from the soma (µm)
G
Sholl interactions apical dendrites
Distance from the soma (µm)
D
Sholl interactions basal dendrites
Distance from the soma (µm)
H
Sholl interactions basal dendrites
Distance from the soma (µm)

Supplemental Figure S4. Dendritic restructuring induced by miR-*Slit1* was confined to proximal dendritic branches. (A) No differences in the soma surface area between the female groups (per group: n=5 animals, 19-22 neurons). **(B)** *Slit1* KD decreased the average basal dendritic arbor length compared to controls. (**C, D)** Scholl analysis revealed no change in branching **(C)** of apical dendritic in vmPFC pyramidal neurons infected with miR-*Slit1* compared to miR-*LacZ*, but a decrease in the branching **(D)** of basal dendrites mainly 60-80 μm from the soma. **(E)** No differences in the soma surface area between the male groups (per group: n=5 animals, 19 neurons). **(F)** *Slit1* KD had no effect on the average basal dendritic arbor length. (**G, H)** Scholl analysis revealed an increase in the branching **(G)** of apical and basal **(H)** dendrites mainly 40-140 μm from the soma. *p<0.05, **p<0.01. Data are shown as means ± s.e.m.

Supplemental Methods

Human brain postmortem tissue

Human postmortem brain tissue and RNA-seq data from MDD and control subjects were collected, analyzed, and reported as part of a published study (1). Briefly, brain tissue was obtained from the Douglas Bell Canada Brain Bank Québec. Males and females were group-matched for age, pH, and BMI. Forty-eight subjects were recruited, and tissue was collected from six brain regions including the anterior cingulate gyrus 25 (BA25; cg25; vmPFC), orbitofrontal cortex (OFC; BA11), dorsolateral PFC (BA8/9; dlPFC), anterior insula (aINS), nucleus accumbens (NAc), and ventral subiculum (vSUB). The study was approved by the research ethics boards of McGill University and Douglas Hospital. Psychiatric history and socio-demographics were obtained for both cases and controls by "psychological autopsies" using DSM-IV criteria by means of SCID-I adapted interviews. vmPFC cDNA from this cohort was used to assess *Slit1* mRNA levels.

Animals

C57BL/6J female and male mice (8-weeks old) (Jackson Laboratory, Bar Harbor) were used for all experiments and habituated to the animal facility for 1 week before experimental manipulations. Mice were housed in groups of 5 at room temperature (24 ± 1 °C) under a 12-hour light/dark cycle (lights on from 7:00 A.M.) with *ad libitum* access to water and food, except when otherwise specified for behavioral testing. Experiments were conducted in accordance with guidelines of the Society for Neuroscience and the Institutional Animal Care and Use Committee (IACUC) at Mount Sinai. Female estrous cycle was monitored by microscopy of vaginal smears at the end of all experiments and confirmed that the large majority of mice were in diestrus.

Viral constructs design, cloning, and validation

Knockdown (KD) constructs designed to target *Slit1* mRNA were cloned using BLOCK-iT Pol II miR RNAi kit (Invitrogen, Carlsbad, CA). Two artificial microRNA (miRNA) oligonucleotides were designed using Invitrogen's RNAi Designer (www.invitrogen.com/rnai) to KD *Slit1* and cloned into pcDNA6.2-GW and further Gateway cloned (Invitrogen, Carlsbad, CA) into the p1005+ herpes simplex viruses (HSV) vector. Mouse neuroblastoma (N2a) cells were transfected using Lipofectamine 2000 (Invitrogen, Carlsbad, CA) with miR-*Slit1* to test the efficacy to downregulate mRNA levels. Results were assessed using qRT-PCR. The sequences of the primers used for the generation of the artificial miRNAs were 5'- TGC TGA TAA CTA ACA CGG ACA TGG CCG TTT TGG CCA CTG ACT GAC GGC CAT GTG TGT TAG TTA T-3' and 5' CCT GAT AAC TAA CAC ACA TGG CCG TCA GTC AGT GGC CAA AAC GGC CAT GTC CGT GTT AGT TAT C-3'. Similarly, the commercial miRNA targeting the *LacZ* gene, which is not expressed in mice, was cloned and used as control. These HSV vectors infect neurons only.

RNAscope® fluorescence in situ hybridization

For *Slit1* mRNA in situ analysis, brains of female mice were collected following cervical dislocation and rapid flash freezing using isopentane/dry ice and immediately placed on dry ice. Coronal sections were obtained using a cryostat (Leica CM 1850, Wetzlar, Germany) at 25 µm thickness and mounted directly on SuperFrost Plus Slides (Thermo Fisher Scientific, Waltham, MA). RNAscope® Multiplex Fluorescent v2 Assay (Advanced Cell Diagnostics, Newark, CA) was used according to the manufacturer's protocol. The following probes were used: mm-Slit1-C1 (catalog number: 502491), mm-glutamic acid decarboxylase 2 (Gad2)-C2 (catalog number: 415071-C2), mm-vesicular glutamate transporter 2 (Slc17a6)-C3 (catalog number: 319171-C3). Staining was visualized within two weeks using a Zeiss (Oberkochen, Germany) LSM 780 confocal microscope at 63x magnification. mRNA puncta were quantified using CellProfiler Analyst 2.2.1 (2).

Stereotaxic surgeries and viral gene delivery

Slit1 KD in the vmPFC was accomplished by injecting HSV vectors expressing a miRNA targeting *Slit1*, as well as green fluorescent protein (GFP) (miR-*Slit1*). As a control, HSV–miRNA-GFP targeting *LacZ* was used (miR-*LacZ*). Mice were anesthetized using a mixture of ketamine (10mg/kg) and xylazine (1 mg/kg). For viral delivery, the following stereotaxic coordinates were applied: +1.8 mm (anterior/posterior), +0.75 mm (medial/lateral), -2.7 mm (dorsal/ventral) at an angle of

15° from the midline (relative to Bregma). A total of 0.5 µl of HSV solution was delivered bilaterally over a 5-minute period (0.1µl/min), followed by 5 minutes of rest after which the needle was slowly removed.

Stress paradigm
The chronic variable stress (CVS) paradigm consisted of repeated daily exposure to one of three different stressors over a period of 21 consecutive days (3). The stressors used were: 100 random mild foot shocks at 0.45 mA for 1 hour, tail suspension for 1 hour, and restraint stress by placement in ventilated 50 mL falcon tube for 1 hour within the home cage. The RNA-seq results and samples from mice exposed to 21 days of CVS used in this study were part of our published study (4).

For subthreshold chronic variable stress (sCVS), female mice were subjected to 3-days of the stressors mentioned above, while male mice were subjected to 6 days of stress (4). This differences in length of the stress exposure between the sexes is due to the greater sensitivity of females compared to males in response to these types of stress (3). This version of sCVS is insufficient by itself to induce stress-related behavioral abnormalities, but when combined with viral-mediated modification of certain genes can reveal altered stress susceptibility (3). Mice were all single caged after completion of the sCVS procedure.

Behavioral testing
Behavior was assessed on day 4 or 7 (post-surgery) in the novelty suppressed feeding (NSF) test, sucrose preference (SP) test, marble burying (MB) test, and forced swim test (FST). Prior to testing, mice were given 60 minutes to acclimate to the testing room. Results were manually assessed by a researcher blind to the experimental groups. The behavioral experiments were repeated in three independent cohorts.

Novelty suppressed feeding (NSF)
The NSF test elicits conflicting motivations in mice: the drive to eat vs. the fear of moving to the center of a novel open arena (5). Mice were food restricted for 24 hours prior to testing (6). Under red-light conditions, mice were placed in the corner of a clear plastic testing chamber (50 x 50 x 20 cm) which was lined with corncob bedding. A single food pellet was present in the center of the box. The latency to begin consumption in a 6-min test was measured. Additionally, home cage latency to feed was measured in a 5-min posttest to confirm that gene manipulation had no effect on appetite.

Sucrose preference (SP)
A core symptom of MDD is a reduced ability to experience pleasure (anhedonia), which can be modeled in rodents in reduced preference for sweetened drinks. In the SP test, mice were given the choice between two bottles with either water or a 2% sucrose solution, which were weighted daily for three days (7, 8). Sucrose preference was calculated by determining the percentage of total sucrose consumption divided by total liquid consumption (sucrose volume/total volume × 100).

Marble burying (MB)
Twenty glass marbles (14 mm diameter) were evenly placed on top of corncob bedding in a standard plexiglass mouse cage. Thereafter, mice were placed individually in the cage for a 15-min period. The experiment was performed under red light. The amount of marbles partly or fully buried were manually scored by a researcher blind to the experimental groups. Mice that have higher levels of anxiety-like behavior tend to bury larger numbers of marbles (9).

Forced swim test (FST)
Mice were placed in a 4 L Pyrex glass beaker containing 3 L of water (25 ± 1 °C) for 6 min (10). Time spent immobile, a measure of passive coping with stress, during the test was determined using EthoviosionXT (Noldus, Wageningen, The Netherlands) video tracking software. The experiment was performed under white light.

Electrophysiology
Recordings were made from vmPFC pyramidal neurons of male and female mice (13 ± 3 weeks old) the day after miR-*LacZ* or miR-*Slit1* injection into vmPFC *in vivo*. Mice were deeply anesthetized with isoflurane and decapitated. The

brains were rapidly removed and chilled in cutting artificial CSF (ACSF) containing (in mM): N-methyl-D-glucamine 93, HCl 93, KCl 2.5, NaH_2PO_4 1.2, $NaHCO_3$ 30, HEPES 20, glucose 25, sodium ascorbate 5, thiourea 2, sodium pyruvate 3, $MgSO_4$ 10, and $CaCl_2$ 0.5; pH 7.4. Chilled brains were embedded in 2% agarose and coronal slices (200 µm thick) were made using a Compresstome (Precisionary Instruments, Natick, MA). Brain slices were allowed to recover at 33 ± 1 °C in cutting solution for 30 minutes and thereafter at room temperature in holding ACSF, containing (in mM): NaCl 92, KCl 2.5, NaH_2PO_4 1.2, $NaHCO_3$ 30, HEPES 20, glucose 25, sodium ascorbate 5, thiourea 2, sodium pyruvate 3, $MgSO_4$, and $CaCl_2$ 2; pH 7.4. After at least 1 hour of recovery the slices were transferred to a submersion recording chamber and continuously superfused (2-4 mL/min) with ACSF containing (in mM): NaCl 124, KCl 2.5, NaH_2PO_4 1.2, $NaHCO_3$ 24, HEPES 5, glucose 12.5, $MgSO_4$ 2, and $CaCl_2$ 2; pH 7.4. All extracellular solutions were at pH 7.3 and 300-310 mOsM and were continuously bubbled with 95% O_2/5% CO_2. Neurons in the vmPFC were visualized using an Olympus BX51WI (Tokyo, Japan) with differential interference contrast optics and infrared illumination. Whole-cell recordings from GFP-positive cells, using 2.5-3.5 MΩ pipettes containing: (in mM: 115 Cs-gluconate, 10 HEPES, 0.1 EGTA, QX-314-Cl, 2.5 MgATP, 0.1 Na-GTP, pH 7.2, 285-287 mOsM). Miniature excitatory postsynaptic currents (mEPSCs) were recorded at a holding potential of -80 mV beginning 2-3 minutes after breakthrough using a Multiclamp 700B amplifier (Axon Instruments). mEPSCs were recorded in ACSF containing picrotoxin (50 µM) and tetrodotoxin (1 µM). Only cells with stable input resistances measured before and after the gap-free period were included in the analysis. Template-based event detection was performed using Clampfit 11.1 (Molecular Devices, San Jose, CA). Templates were generated by averaging 20 events and the automated search results were verified manually. The peak amplitudes and inter-event intervals were collected for mEPSC recordings, and the first 150 events were analyzed. Recordings and analyses were conducted in a blinded fashion.

Immunohistochemistry and dendritic morphology analysis

Female and male mice received bilateral injections of HSV vectors expressing miR-*LacZ* or miR-*Slit1* in their vmPFC. Four days after infection, mice were anesthetized and perfused intracardially with PBS, followed by cold 4% paraformaldehyde (PFA) in PBS. Brains were removed, post-fixed in the same fixative overnight, and transferred to PBS 24 hours later. Coronal sections (100 µm) were obtained on a vibratome (Leica VT 1000S, Wetzlar, Germany) and stored in 0.01% sodium azide. Sections were washed in PBS, permeabilizated in 0.2% Triton, saturated in 3% Donkey Serum and 0.2% Triton, and washed again in PBS. Slides were incubated overnight with their primary antibody (Anti-GFP, 1/500) (Jackson ImmunoResearch, West Grove, PA) at room temperature. Samples were washed and incubated with their secondary antibody (Alexa 488 Donkey anti-Chicken, 1/500 (Jackson ImmunoResearch, West Grove, PA). They were washed, nuclei were stained using DAPI, and slides received a final wash before they were mounted and covered with Prolong diamond antifade mountain (Thermo fisher scientific, Waltham, MA). A total of 19 to 22 pyramidal neurons per group were reconstructed and visualized using a Zeiss (Oberkochen, Germany) Immersol 518F fluorescence microscope at 40x magnification. Pyramidal neurons were defined by the presence of a distinct, single apical dendrite and a minimum of three basal dendrites. GFP-positive pyramidal cells within layer II-III of the vmPFC were manually traced with a virtual pen using Neurolucida 11.09. Using this trace, NeurolucidaExplorer calculated morphological properties (total apical and basal dendritic length, apical and basal dendritic branchpoints, average basal dendritic length, and performed Scholl analysis). For Scholl analysis, a 20 µm radius interval was used. All neuronal tracing and analysis were conducted in a blinded fashion.

Microdissection, RNA isolation, and qRT-PCR

Brain microdissections were collected from mice that were euthanized by cervical dislocation. Brains were coronally sectioned using a brain matrix into 1 mm-thick slices. A 14G blunt needle was used for microdissection of the vmPFC. Viral expression and placement were confirmed using an epifluorescence microscope.

Total RNA was purified from the tissue using the RNeasy micro kit (Qiagen, Germantown, MD) and TriZol. Samples were treated with DNAse I and concentration and purity were tested using NanoDrop (Thermo Fisher Scientific, Waltham, MA).

For quantitative real time-PCR (q-PCR), a total of 500ng RNA was converted to cDNA using iScript (Bio-Rad Laboratories, Herculus, CA). qPCR reactions were run in triplicates using QuantStudio 7 qPCR machine (Thermo Fisher

Scientific, Waltham, MA) using Sybr Green (Applied Biosystems, Foster City, CA). *Slit1* expression was analyzed using the following primers in mouse, F: 5'-GCC ATC CAG ACA CTG CAT CT-3'; R: 5'-CTG CCA GCC ACT TGA GGT TA-3'; and human F: 5'-GAG GTG CTG ACC CTG AAC AA-3', R: 5'-CCG TAG CTT GGG CAT ATG GT-3' in comparative ΔΔCt method and normalized to a housekeeping gene (*Hprt1*) (Mouse primers, F: 5'-GCA GTA CAG CCC CAA AAT GG-3'; R: 5'-GGT CCT TTT CAC CAG CAA GCT-3'; Human primers, F: 5'-GAC TAA TTA TGG ACA GGA CTG AAC GTC-3; R: 5'-TCT CCT TCA TCA CAT CTC GAG C-3'). See Supplemental Table 1 for Ct values of *Hprt1*.

RNA sequencing and data analysis

Libraries were prepared from 7 individual female mice per group using the TruSeq Stranded Total RNA Library Prep Gold (Illumina, San Diego, CA) from virally infected mPFC tissue at baseline or after 3 days of sCVS. Briefly, 1 µg ribosomal depleted RNA was converted to cDNA using random hexamers. Adapters were ligated and samples were size selected with AMPure XP beads (Beckman Coulter, Brea, CA). Barcode bases of 6 bp were introduced at one end of the adapters during PCR amplification steps. Quality and concentration of libraries were analyzed with a Bioanalyzer DNA 1000 chip (Agilent, Santa Clara, CA). 7 samples were pulled per lane for multiplexing and sequenced on an Illumina Hi-Seq machine with 260 bp paired-ends reads by Genewiz (South Plainfield, NJ) and gave rise to ~35 million reads per sample.

For RNA sequencing (RNA-seq) differential expression analysis, raw reads were aligned to the mouse genome (HISAT2 mm10) (11) for mouse vmPFC. Counts of reads mapping to genes were obtained using featureCounts software of Subread package against Ensembl v90 annotation (12). Quality control (QC) was performed using FastQC (13) and principal component analysis was used to identify outliers. Normalization and differential expression analysis were performed using DESeq2 (14). Raw data was deposited in GEO (GSE158993). Heatmaps were generated using Morpheus (https://software.broadinstitute.org/morpheus), and gene ontology (GO) analysis was performed using Enrichr (15). Ingenuity Pathway Analysis (IPA) (Qiagen, Germantown, MD) was performed to identify predicted upstream regulators. Differentially expressed gene lists can be found in Supplemental Table 2.

Statistical analysis

GraphPad Prism 8.0 software package was used for analyzing the data. For all experiments comparing two groups between-subjects t-tests were used, and Two-way ANOVA were used for experiments with 2X2 design, with subsequent post hoc Tukey tests. Outliers were detected and removed according to the Grubbs outlier test. $P<0.05$ was used as cutoff for significance.

Supplemental Table S1. HPRT1 CT values.

	Group	HPRTlCT	Statistical analysis
Human	Female Control Female MDD Male Control MaleMDD	23.29 23.08 22.51 22.87	Two-way ANOVA, Fgender(l,35)=5.329, p=0.0407) nothing in Tukey Post-hoc
Mice	Female Control Female 21d CVS Male control Male 21d CVS	24.58 24.24 24.68 24.11	Two-way ANOVA, Fstress(I,33)=4.858, p=0.0346) nothing in Tukey Post-hoc
Female HSV validation	Lacz Slitl	24.18 23.62	(tc32)= 1.657, p=0.1073)
Male HSV validation	Lacz Slitl	24.08 22.47	(tc21)=0.8555, p=0.4019)

Supplemental Table S2. RNA-seq DEG list.
See Supplement 2 (Excel file).

Supplemental Table S3. GO term related genes.
See Supplement 2 (Excel file).

Supplemental Table S4. IPA results.
See Supplement 2 (Excel file).

Supplemental References

1. Labonté B, Engmann O, Purushothaman I, Menard C, Wang J, Tan C, et al. Sex-specific transcriptional signatures in human depression. Nat Med. 2017;23(9):1102-11.
2. Jones TR, Kang IH, Wheeler DB, Lindquist RA, Papallo A, Sabatini DM, et al. CellProfiler Analyst: data exploration and analysis software for complex image-based screens. BMC Bioinformatics. 2008;9:482.
3. Hodes GE. Sex differences in nucleus accumbens transcriptome profiles associated with susceptibility versus resilience to sub-chronic variable stress. Journal of Neuroscience. 2015;35(50):16362–76.
4. Labonté B, Engmann O, Purushothaman I, Menard C, Wang J, Tan C, et al. Sex-Specific Transcriptional Signatures in Human Depression. Nature Medicine. Under review
5. David DJ, Samuels BA, Rainer Q, Wang JW, Marsteller D, Mendez I, et al. Neurogenesis-dependent and -independent effects of fluoxetine in an animal model of anxiety/depression. Neuron. 2009;62(4):479-93.
6. Santarelli L. Requirement of hippocampal neurogenesis for the behavioral effects of antidepressants. Science. 2003;301:805-9.
7. Vialou V. Serum response factor promotes resilience to chronic social stress through the induction of DeltaFosB. J Neurosci. 2010;30:14585-92.
8. Krishnan V. Molecular adaptations underlying susceptibility and resistance to social defeat in brain reward regions. Cell. 2007;131:391-404.
9. Thomas A, Burant A, Bui N, Graham D, Yuva-Paylor LA, Paylor R. Marble burying reflects a repetitive and perseverative behavior more than novelty-induced anxiety. Psychopharmacology (Berl). 2009;204(2):361-73.
10. LaPlant Q. Dnmt3a regulates emotional behavior and spine plasticity in the nucleus accumbens. Nat Neurosci. 2010;13:1137-43.
11. Kim D, Paggi JM, Park C, Bennett C, Salzberg SL. Graph-based genome alignment and genotyping with HISAT2 and HISAT-genotype. Nat Biotechnol. 2019;37(8):907-15.
12. Liao Y, Smyth GK, Shi W. The R package Rsubread is easier, faster, cheaper and better for alignment and quantification of RNA sequencing reads. Nucleic Acids Res. 2019;47(8):e47.
13. Andrews A. FastQC: a quality control tool for high throughput sequence data. 2010 [Available from: https://www.bioinformatics.babraham.ac.uk/projects/fastqc/.
14. Love MI, Huber W, Anders S. Moderated estimation of fold change and dispersion for RNA-seq data with DESeq2. Genome Biol. 2014;15(12):550.
15. Chen EY, Tan CM, Kou Y, Duan Q, Wang Z, Meirelles GV, et al. Enrichr: interactive and collaborative HTML5 gene list enrichment analysis tool. BMC Bioinformatics. 2013;14:128.
16. Zhang Y, Chen K, Sloan SA, Bennett ML, Scholze AR, O'Keeffe S, et al. An RNA-sequencing transcriptome and splicing database of glia, neurons, and vascular cells of the cerebral cortex. J Neurosci. 2014;34(36):11929-47.
17. Zhang Y, Sloan SA, Clarke LE, Caneda C, Plaza CA, Blumenthal PD, et al. Purification and Characterization of Progenitor and Mature Human Astrocytes Reveals Transcriptional and Functional Differences with Mouse. Neuron. 2016;89(1):37-53.
18. Kozlenkov A, Wang M, Roussos P, Rudchenko S, Barbu M, Bibikova M, et al. Substantial DNA methylation differences between two major neuronal subtypes in human brain. Nucleic Acids Res. 2016;44(6):2593-612.
19. Zeisel A, Muñoz-Manchado AB, Codeluppi S, Lönnerberg P, La Manno G, Juréus A, et al. Brain structure. Cell types in the mouse cortex and hippocampus revealed by single-cell RNA-seq. Science. 2015;347(6226):1138-42.